

Electromechanical Analyses of a Small BLDC Motor for a Surgical Device

Mingzhe Li, Cheol Kim*, and Se-Ho Kwak

Abstract—A small BLDC motor is under consideration to operate small dental and surgical hand-pieces instead of low torque air turbines, due to high torque density compared to a size. Electromagnetic analyses were carried out numerically in order to improve the performance of a hand-piece motor such as torque output and torque ripple. Several case studies on the characteristics of electromagnetic torque outputs were carried out by increasing numbers of coil wires from 11 to 30 wound and the maximum motor torque was obtained with 20 wound wires at the electromagnetic angle of 90°. The stator slot made of Teflon was found to be better than steel in the magnetic flux density from a material comparison study. In an effort to reduce torque ripple of the motor, the changes in torque ripples for several slot shapes of a stator were evaluated by finite element analyses and compared. The slot with both circular holes and V-cut showed a best ripple performance that was 6.10%, compared to 7.80% of the current design.

Keywords— BLDC Motor, Motor Torque, Medical Hand-piece, Stator Coil, Ripple, Finite Element Method.

I. INTRODUCTION

THE small hand-pieces have been widely used to cure diseased teeth and tissues during various dental and surgical operations [1-3]. Most dental hand-pieces have adopted an air-turbine as a driving engine for last 30 years [4-9]. The hand-piece driven by an air-turbine, however, has a difficulty to obtain enough output torque and sometimes stops to rotate due to contamination of burrs. Recently, the research is underway to replace the air-turbine by a series of a gear train with an electric motor. The brushless direct current (BLDC) motor is widely used in various industries because it has a long life, low noise, higher speed and higher torque, and is made easily smaller. The new hand-piece under development consists of a small driving BLDC motor, a small high speed gear train and a small burr. The mating gears usually rotate at 50,000 - 200,000 rpm in order to transfer power to the end of a burr by way of a series of high-speed gear train. Because BLDC motors have several advantages over general brushed DC or induction motors, including more torque per weight, more torque per watt, increased reliability, reduced noise, longer lifetime (no

brush and commutator erosion), elimination of ionizing sparks from the commutator, and overall reduction of electromagnetic interference, its applications are very broad in various industries [10-12].

Structural optimization was performed for magnetic devices in a magnetic field using a homogenization method [13-15]. A new configuration of a brushless DC motor without a permanent magnet was studied by finite element analysis [16]. A design method of a single-phase brushless DC fan motor was studied to obtain optimal driving efficiency [17]. In addition, the research on the reduction of torque ripple was performed for synchronous reluctance motor using an asymmetric flux barrier arrangement [18]. Taguchi optimization method was applied in an effort to reduce torque ripple in interior permanent magnet motor [19]. The shape design of a hole in a motor rotor was carried out by drilling axial circular holes of optimal radius and position in the flux path of the rotor core. The torque curves of the optimized motor showed lower pulsating torque and higher average torque [20]. Structural optimization based on the level set method was formulated to reduce torque ripples by minimizing the difference between torque values at defined rotor positions and the constant target average torque value under the constrained material usage [21]. A new optimization technique was applied to design the rotor of interior permanent magnet motor which consists of a permanent magnet and ferromagnetic material for reducing the torque ripple. To express three different material properties (PM, FM, and air), a multi-phase level-set model representing two level-set functions was introduced and the concept of a phase-field model was incorporated to distribute level-set functions for controlling the complexity of the structural boundaries [22].

There are little studies on the performance analyses of high speed small BLDC motors especially used for various medical hand-pieces for many kinds of medical operations. In this study, electromagnetic analyses have been performed using MAXWELL program in order to improve the torque outputs of the hand-piece BLDC motor. The electromagnetic numerical results have been compared with measured ones. Variations in motor torques were calculated according to changes in the number of winding coils and then the number of coils that can increase torque outputs was determined. In addition, the study on torque ripple was also done to obtain a good slot shape of a stator which could give lower torque ripple. The torque ripple refers to a periodic increase or decrease in output torque as the output shaft rotates. It is measured as the difference in

M. Lee is with Hyundai Motor Co., Yantai, China (e-mail: limingzhe19880708@live.cn).

*C. Kim is with Kyungpook National University, Daegu, 702-701 Korea. (corresponding author: +82-53-950-6586; fax: +82-53-950-6550; e-mail: kimchul@knu.ac.kr).

S. H. Kwak is with R & D Center, Saeshin Precision Co., Ltd., Daegu, 711-814 Korea (e-mail: seho5000@saeshin.com).

maximum and minimum torque over one complete revolution, generally expressed as a percentage.

II. MOTOR TORQUE ANALYSIS

Fig. 1 shows a surgical hand-piece and a BLDC motor assembly that is composed of a sensor, a rotor and a stator. The reference BLDC motor (which is an existing design) for this study has a diameter of 20 mm and a length of 30.0 mm. The sensor controls the flow of an electric current by sensing a sequence, a position and a speed of the rotor. The rotor consists of a rotating shaft and a Nd-Fe-B permanent magnet with S and N poles, and the stator is composed of coils, slots, and a cover. As an electric current run through the coil, an electromagnetic force occurs. Coils, slots and a cover are made of brass, Teflon and steel, respectively. The locations of key parts in the stator and the rotor are described in Fig. 2.

In Fig. 3, three bunches of coils denoted as 1, 2 and 3 that are located in a pair with the angle of 180° in opposite directions and a permanent magnet in the central region are represented. As the rotor spins, the current in stator coils varies and the direction of an electromagnetic field also changes. Because the 3-phase current is applied to operate the motor, only through two coils current flows and no current in the rest of coils.

Fig. 4 shows how two directions of electromagnetic forces varies as electric current path shifts from coil to coil wound at the stator and the magnet rotor at the center rotates in 1/4 cycle. The direction of electromagnetic forces produced by the magnet is denoted by a dotted arrow and coils by a solid arrow respectively, where the “x” denotes current in and “•” denotes current out.

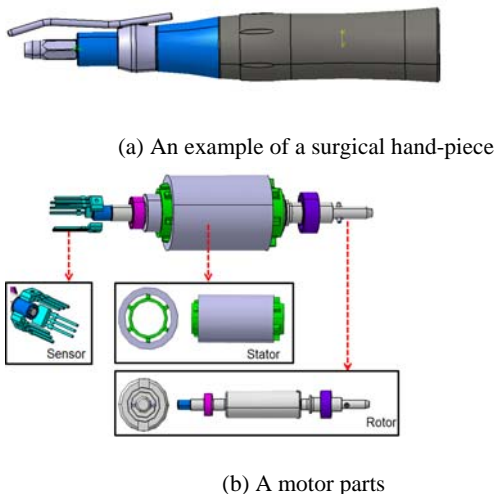


Fig. 1 A BLDC motor assembly and its parts used for a small surgical hand-piece

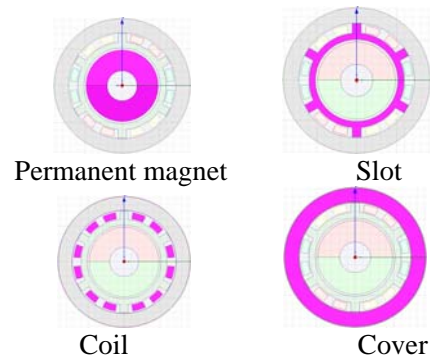
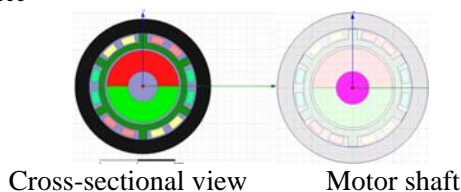


Fig. 2 Locations of key parts in the cross-section of the reference stator and rotor



Fig. 3 Three coils (1, 2 and 3) and a permanent magnet in the cross-section of a BLDC motor

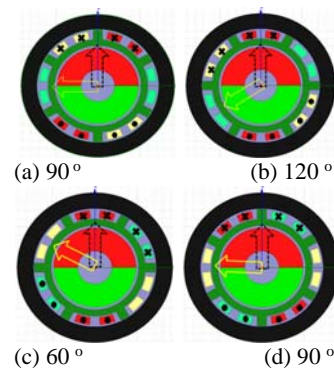


Fig. 4 Directions of electromagnetic forces produced by the magnet (dotted arrow) and coils (solid arrow), where the “x” denotes current in and “•” denotes current out

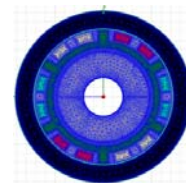


Fig. 5 FE model of a BLDC motor

A direction of an electromagnetic force produced by the central magnet is denoted as a dotted arrow and that by stator coils is represented by a solid arrow. The marks “x” and “•” at slots denote current in and out, respectively. Figs. 4(a), (b), (c) and (d) show the angles between two electromagnetic forces- 90°, 120°, 60° and 90°.

The angle between the magnetic field directions of a rotor and a stator always exists between 60 and 120 degrees. The largest motor torque occurs at 90 degree and the smallest torque occurs at 60 or 120 degree. The largest and smallest torques were calculated using MAXWELL 2-D.

Fig. 5 shows a finite element model of a BLDC motor constructed by 3-noded elements. The vector potential at the outer circumference of the motor cross-section was set to be zero. The coercive force of the magnet is 10,500 Oe (Oersted) and the remanence is 14,000 Gauss. The rotor and a cover are made of SUS303F which magnet permeability is 1.008. As the current of 2.5A runs through a coil and 12 coils are wound around a slot, the total current is 30A. The slot is made of Teflon material which relative permeability is 1.0.

The magnetic flux density is the largest at both sides as shown in Fig. 6. The maximum motor torque on the magnetic rotor was 21.50 N-mm at 90° in-between stator and rotor electromagnetic forces. The torque per meter (m) produced in the permanent magnetic was originally calculated as 717.0 N-m and if the length of 0.03 m is multiplied, then the total torque ends up with 21.50 N-mm. The minimum torque was 19.95 N-mm at 60° or 120°. The torque per meter was originally calculated as 665.0 N-m at 60° and 120°. As a result, the computed average torque of max. and min. values is 20.725 N-mm. The average measured torque of a real DLDC motor is 20.46 N-mm at 28,000 rpm and 60W of a power output. The numerical analysis predicts the torque output accurately, compared with experiments.

A parametric study was performed in an effort to improve the torque output by changing the number of coils and the shape and material of a stator. The torque outputs of the BLDC motor were calculated on the basis of the cross-sectional area of one coil, as the number of coils increases. To add more coils, more space is required without increase in a motor diameter. The outer diameter of the motor and R1 (= 5.95 mm) in Fig. 7 are, therefore, fixed and Rx can increase from 7.225 mm to R_{max} = 9.175 mm in order to secure more space for coils.

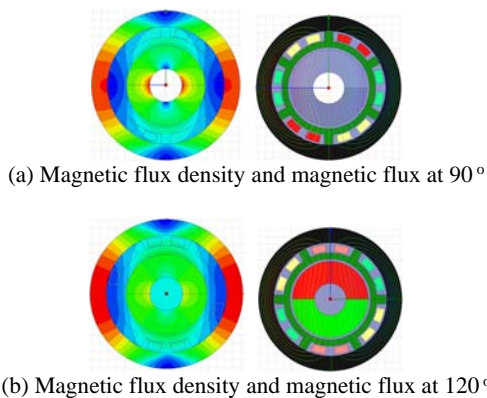


Fig. 6 Distribution of a magnetic flux density and magnetic flux in cases of 90° and 120° in-between 2 electromagnetic forces

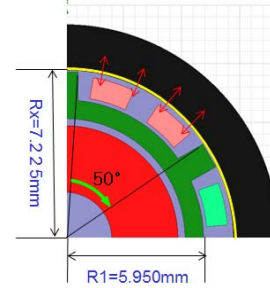


Fig. 7 Dimensions of a quarter motor

The area of a single coil cross-section is 0.513 mm² and one slot occupies 50°. The two bunches of coils in the angle of 50° are placed as shown in Fig. 7. The number of coils can be related with the space parameter, Rx, as in Eq. (1).

$$0.153\text{mm}^2 \times \text{number of coils} = \pi(R_x^2 - R_1^2) \frac{50}{360} \quad (1)$$

Fig. 7 shows a quarter dimensions of a present BLDC motor used for a parametric study. There are 12 coil wires wound in one bunch of coils and the required average cross-sectional area for a single wire is 0.153 mm². The maximum area for all wires is 10.642 mm calculated by using Eq. (1). The motor torque was calculated as the number of coil wires changed at the angles of 60° or 90° between the electromagnetic field directions of a rotor and a stator. The coil area changes proportionally as the number of coil wires varies. The changes in a coil cross-sectional area and Rx with respect to the number of coils at 90° are tabulated in Table 1. Figs. 8(a), (c) and (e) show the cross-section models of the stator and rotor with 11, 20 and 30 coils, respectively. It is noticeable that the cross-sectional areas of the cover structure (i. e., the thickness of the outer circle) in the figure reduce as the internal coil areas increase. Figs. 8(b), (d) and (f) represent the corresponding distribution of magnetic flux densities of Figs. 8(a), (c) and (e) models, respectively.

Table 1. The changes in a coil cross-sectional area and Rx with respect to the number of coils at 90°

No.(coil wires)	Coil area (cross-section) (mm ²)	R ₁ (mm)	R _x (mm)	R _{max} (mm)	A _{max} (mm ²)
12	3.665	5.950	7.225	9.175	10.642
13	3.970		7.321		
14	4.276		7.416		
15	4.581		7.510		
16	4.886		7.603		
17	5.192		7.694		
18	5.497		7.785		
19	5.803		7.874		
20	6.108		7.962		
21	6.413		8.050		
22	6.719		8.136		
23	7.024		8.222		
24	7.330		8.307		

25	7.635	8.390
26	7.940	8.473
27	8.246	8.556
28	8.551	8.637
29	8.857	8.718
30	9.162	8.798
31	9.467	8.877
32	9.773	8.955
33	10.078	9.033
34	10.384	9.110
35	10.689	9.187

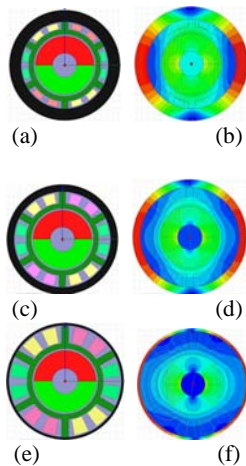


Fig. 8 (a) A model of 15 coils, (b) magnetic flux density of a 15 coil-model, (c) a model of 20 coils, (d) magnetic flux density of a 20 coil-model, (e) a model of 30 coils, and (f) magnetic flux density of a 30 coil-model, all at 90°

As the number of coil wires increases, the area also increases and the thickness of a motor cover decreases. Figs. 9 and 10 show the motor torque outputs per a unit mm calculated by using MAXWELL on the different number of coil wires from 11 to 30 at 60 and 90 degrees. The maximum motor torque was obtained with 20 wound wires in the both cases of electromagnetic angles as shown in Figs. 9 and 10. The trend in torque variations is that the torque increases as the wire number increases up to 20 and then it decreases gradually even though the wire number increases. As expected, the torques at 90° is higher than those at 60°.

As another study to increase the torque output, two different materials, Teflon and steel, for the stator slot were considered at the angle of 90° between electromagnetic field directions of a stator and a rotor. Because that the magnetic permeability of a Teflon slot is smaller than that of a steel slot, the magnetic flux density and the electromagnetic field of a BLDC motor may be changeable. Fig. 11(a-b) shows the distribution of magnetic flux density with a steel slot and magnetic lines of flux with a steel slot at 90°, respectively. It is noticed from Fig. 11(b) that the large magnetic flux density is concentrated near a slot. The torque per meter produced by the steel slot was originally calculated as 543.0 N-m and if the slot length of 0.03 m is

multiplied, then the total torque ends up with 16.29 N-mm, which is 79.6% of Teflon slot torque. The result means that the Teflon slot is better than the steel one.

III. RIPPLE ANALYSIS

A motor torque ripple is defined as the percentage of the difference between the maximum torque and the minimum torques compared to the average torque. It is caused by cogging torque, mechanical imbalances, etc. and occurs due to the variation in torque per one revolution. The torque ripple is evaluated based on the following equation [22],

$$Torque\ Ripple = \frac{T_{max} - T_{min}}{(T_{max} + T_{min}) / 2} \times 100(\%) \quad (2)$$

where T_{max} and T_{min} denote the maximum and minimum torques, respectively.

Torque ripple in electrical motors is generally undesirable, since it causes vibrations and noise, and might reduce the lifetime of the BLDC motor. Extensive torque ripple can require measures such as skewing or changes to the motor geometry that might reduce the general performance of the BLDC motor. In addition to the cogging torque, the torque ripple can be caused due to the interaction between the magneto-motive force (MMF) and the airgap flux harmonics. This MMF ripple can be influenced by variations in the geometry of the motor design, and especially the number of stator slots, the number of poles, the magnet angle, and the slot opening width are important parameters to be investigated.

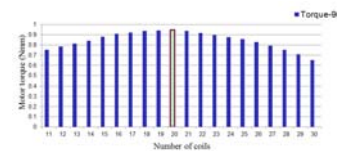


Fig. 9 Motor torque per a unit mm with the different number of coil wires at 90°

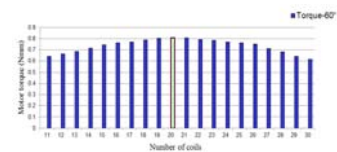


Fig. 10 Motor torque per a unit mm with the different number of coil wires at 60°

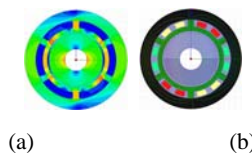


Fig. 11 (a) Distribution of magnetic flux density with a steel slot, and (b) magnetic lines of flux with a steel slot at 90°

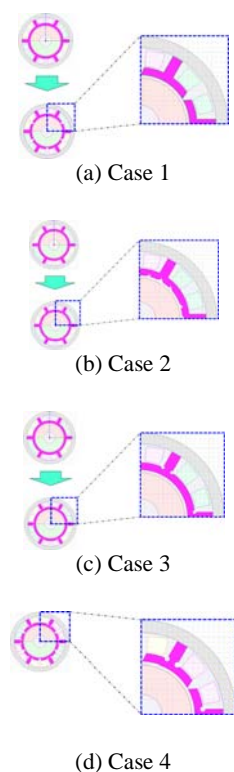


Fig. 12 Four different cases of slot shapes in a state used for computation of the torque ripple

Table 2. Maximum and minimum torques of the four different cases

Case	Maximum torque (90°)	Minimum torque (60°)
1	0.933 Nm	0.815 Nm
2	0.941 Nm	0.806 Nm
3	0.938 Nm	0.812 Nm
4	0.929 Nm	0.821 Nm

In an effort to reduce the torque ripple, four different cases of slot shapes in a stator were designed and the torque ripples were compared. The computed torque ripple for the current slot with 20 coils is 7.8%. The four cases of design changes in a slot configuration are depicted in Fig. 12. The maximum and the minimum torques of the four cases are summarized in Table 2. The torque ripples for cases 1, 2, 3 and 4 are calculated as 6.75%, 7.85%, 7.20%, and 6.10% on the basis of Eq. (2), respectively. The motor slot shape of the case 4 gives least torque ripple among all four cases.

IV. CONCLUSION

Through electromagnetic modelling and analyses, how to improve the torque output of a hand-piece BLDC motor has been studied. The average torque calculated from the existing reference motor was 20.73N·mm and the measured torque was 20.46 N·mm. The analysis method can be thought to be, therefore, accurate from the fact that the numerical result correlates with measured one. In an effort to improve the torque of the reference motor further, some case studies on the

electromagnetic torque were performed regarding to various numbers of coil wires from 11 to 30 wound and the maximum motor torque was obtained with 20 wound wires at the electromagnetic angle of 90°. To reduce the torque ripple of the motor, the changes to torque ripples for several slot shapes in a stator were evaluated and compared. The slot with both circular holes and V-cuts showed a best ripple performance that was 6.10%, compared to 7.80% of the current design.

ACKNOWLEDGMENT

This research was supported by the project of Daegyeong Leading Industry Development for the Economic Regions (2012 -selected).

REFERENCES

- [1] J. E. Dyson, and B. W. Darvel, "The Development of the Dental High Speed Air Turbine Handpiece-Part1", Australian Dental Journal, Vol. 38, No 1, 1993, pp. 49-58.
- [2] J. E. Dyson, and B. W. Darvel, "The Development of the Dental High Speed Air Turbine Handpiece-Part2", Australian Dental Journal, Vol. 38, No 29, 1993, pp. 131-143.
- [3] S. H. Suh, Y. Choi, H. W. Roh, and H. Doh, "Flow Analysis in the Bifurcated Duct with PIV System and Computer Simulation", Trans. of the KSME(B), Vol. 23, No. 1, 1999, pp. 123-180.
- [4] C. Kim, J. Y. Kim, J. H. Lee, and S. H. Kwak, "Strength Analyses of New 2- and 3-axis-type Small Multiplying Gears in Dental Hand-piece", Trans. Korean Soc. Mech. Eng. A., Vol. 36, No. 9, 2012, pp. 1027-1032.
- [5] J. E. Dyson, and B. W. Darvel, "Flow and free Running Speed Characterization of Dental Air Turbine Hand-piece", Journal of Dentistry, Vol. 27, 1999, pp. 456-477.
- [6] M. C. Han, "Development of Ultra High Speed Dental Hand-piece", Trans. of the KSME, 2008, pp. 68-72.
- [7] H. H. Kim, T. J. Je, J. C. Jeon, H. J. Choi, C. E. Kim, K. M. Lee, B. W. Kong, and T. M. Kim, "Study on Precision Balancing Method of BLDC Motor Shaft for the Application of Medical Handpiece", Proceeding of the KSMPE Spring Conference 2013, pp. 133.
- [8] Dyson, J. E. and Darvel, B. W., "Torque, Power and Efficiency Characterization of Dental Air Turbine Handpiece", Journal of Dentistry 27, 1999, pp. 573-586.
- [9] Kong, T. W., Park, S. H., Yu, J. S., Lee, B. K., Won, C. Y., "Drive System of Battery Type Surgical Handpiece", The Korean Institute of Illuminating and Electrical Installation Engineers 2007 Spring, pp. 64-66.
- [10] E. H. E. Bayoumi, and Z. A. Salmeen, "Practical Swarm Intelligent Control Brushless DC Motor Drive System using GSM Technology", WSEAS Trans. on Circuits and Systems, Vol. 13, 2014, pp. 188-201.
- [11] A. H. O. Ahmed, "High Performance Speed Control of Direct Current Motors Using Adaptive Inverse Control", WSEAS Trans. on Systems and Control, Vol. 7, 2012, pp. 54-63.
- [12] R. A. Habibabadi, and A. Nekoubin, "Analysis and Simulation of Single-Phase and two-Phase Axial Flux Brushless DC Motor", WSEAS Trans. on Power Systems, Vol. 8, 2013, pp. 1-11.
- [13] J. Yoo, N. Kikuchi, and J. L. Volakis, "Structural Optimization in Magnetic Devices by the Homogenization Design Method", IEEE Trans. on Magnetics, Vol. 36, No. 3, 2000, pp. 574-580.
- [14] J. Yoo, N. Kikuchi, and J. L. Volakis, "Structural Optimization in Magnetic Fields Using the Homogenization Design Method-Part I", Archives of Computational Methods in Engineering State of the art reviews, Vol. 8, No. 4, 2001, pp. 387-406.
- [15] J. Yoo, N. Kikuchi, and J. L. Volakis, "Structural Optimization in Magnetic Fields Using the Homogenization Design Method-Part II", Archives of Computational Methods in Engineering State of the art reviews, Vol. 9, No. 3, 2002, pp. 257-282.
- [16] H. Moradi, E. Afzai, and F. Faghilhi, "FEM Analysis for a Novel Configuration of Brushless DC Motor without Permanent Magnet", Progress In Electromagnetics Research, PIRE98, 2009, pp. 407-423.
- [17] C. L. Chiu, Y. T. Chen, Y. L. Liang, and R. H. Liang, "Optimal Driving Efficiency Design for the Single-Phase Brushless DC Fan Motor", Progress In Electromagnetics Research, PIRE98, 2010, pp. 407-423.
- [18] M. Sanada, K. Hiramoto, S. Morimoto, and Y. Takeda, "Torque Ripple Improvement for Synchronous Reluctance Motor using an Asymmetric Flux Barrier Arrangement", IEEE Trans. Ind. Appl., Vol. 40, No. 4, 2004, pp. 1076-1082.
- [19] S. I. Kim, J. Y. Lee, Y. K. Kim, J. P. Hong, Y. Hur, and Y. H. Jung, "Optimization for Reduction of Torque Ripple in Interior Permanent Magnet Motor by Using the Taguchi Method", Magnetics, IEEE Transaction on, Vol. 41, No. 5, 2005, pp. 1796-1799.
- [20] K. Kioumars, M. Moallem, and B. Fahimi, "Mitigation of Torque Ripple in Interior Permanent Magnet Motor by Optimal Shape Design", Magnetics, IEEE Transaction on, Vol. 42, No. 11, 2006, pp. 3706-3711.
- [21] J. Kwack, S. Min, and J. P. Hong, "Optimal Stator Design of Interior Permanent Magnet Motor to Reduce Torque Ripple Using the Level Set Method", Magnetics, IEEE Transaction on, Vol. 46, No. 6, 2010, pp. 2108-2111.
- [22] S. Lim, S. Min, and J. P. Hong, "Low Torque Ripple Rotor Design of the Interior Permanent Magnet Motor Using the Multi-Phase Level-Set and Phase-Field Concept", IEEE Transactions on Magnetics, Vol. 48, No. 2, 2012, pp. 907-910.